2011 American Control Conference
on O'Farrell Street, San Francisco, CA, USA
June 29 - July 01, 2011

Experimental Validation of a Scaled Instrument for Real-time Hybrid Testing

Xiuyu Gao, Nestor E. Castaneda, Shirley J. Dyke, Sisu Xi, Christopher D. Gill,
Chenyang Lu and Yasuki Ohtori

Abstract—**A highly reconfigurable cyber-physical Real-time Hybrid Test (RTHT) instrument is under development that is particularly suitable for Civil Engineering structural control testing applications. The instrument serves as a testbed for studying structural system behavior under dynamic loading and associated vibration mitigation control techniques. The focus of this paper is to validate the developed framework experimentally regarding both its accuracy and efficiency in conducting RTHT. A MATLAB-based nonlinear finite element simulation tool, designed to predict seismically excited non-linear building response, is used as an analytical substructure, with a magneto-rheological (MR) damper as a physical substructure. A model based control scheme is adopted to compensate for de-synchronization between substructure interfaces caused by hydraulic actuator dynamics. The RTHT is then conducted for both passive and semi-active MR damper control cases, the results of which show an excellent match between RTHT and pure numerical simulation outputs, thus demonstrating the effectiveness of the prototype instrument.**

I. Introduction

Two methodologies are commonly used for evaluating the performance of structural systems when subjected to earthquake loads: the shake table test and the so called pseudo-dynamic test (PSD). Although more realistic motions can be achieved through a shake table test, only reduced-scale structural models are usually tested due to the payload constraints of the shake table. Alternatively, in PSD tests, the structural specimen is subjected to a set of displacement increments that are sequentially imposed by the use of hydraulic actuators. Within each loading step, force signals measured from the test specimen are fed back into a numerical integration scheme to solve the equation of motion and calculate the next displacements to be imposed. However, the suitability of PSD for testing velocity dependent devices (e.g. dampers) is limited due to their expanded time scale execution. Consequently, continuous or real-time strategies for PSD tests, in which a one-to-one time scale for experiment-to-simulation execution is achieved, are desirable to reproduce more realistic motions.

Manuscript received September 22, 2010. This work was supported in part by the U.S. National Science Foundation under Grant CNS-1028668 (MRI), CMMI-1011534 (NEESR) and Purdue University Cyber Center Special Incentive Research Grant (SIRG).

X. Gao, N. E. Castaneda and S. J. Dyke are with Purdue University, West Lafayette, IN 47906 USA (e-mail: {xygao, ncastan, sdyke}@ purdue.edu).

S. Xi, C. D. Gill and C. Lu are with Washington University, St. Louis, MO 63130 USA. (e-mail: xisisu@gmail.com, {cdgill, lu}@cse.wustl.edu).

Y. Ohtori is with Central Research Institute of Electric Power Industry, JAPAN. (email: ootori@criepi.denken.or.jp)

Hybrid testing techniques can also be integrated with PSD test implementations to reduce the cost involved with fabrication and full-scale testing of large-scale structures. Within a hybrid test implementation, critical components of the structural system under evaluation can be physically tested to be better understood, while others (e.g., more predictable ones) can be represented with computational models. As a result, a real-time hybrid test (RTHT) implementation provides a suitable platform to evaluate structural / rate-dependent systems under actual dynamic and inertial conditions without requiring whole system testing.

Some PSD and RTHT platforms can be found currently through the George E. Brown Network for Earthquake Engineering Simulation. One of the NEES Facilities is entirely focused on this technology to advance our ability to achieve resilience in our communities. The RTMD NEES facility at Lehigh University (http://www.nees.lehigh.edu) has been leading the development of this technology and provides capabilities to use these methods to advanced testing of structural systems. An in depth description of this project and other implementations from different NEES facilities can be found at the NEES web site: (http://www.nees.org).

The main objective of this paper is to introduce and present preliminary experimental results of a scaled RTHT framework that is currently being implemented at the Intelligent Infrastructure Systems Laboratory (IISL) at Purdue University. The implementation is primarily aimed for structural control applications. Therefore, an experimental setup with a physical MR damper along with an analytical building model is used to validate the accuracy and efficiency of the proposed RTHT framework. This paper is organized in three main sections. Components and mathematical background of the RTHT framework are introduced in Section II. Section III describes the experimental setup components. Physical substructure characterization and the design of the analytical substructure are also described in Section III. Finally, Section IV presents validation results for the RTHT implementation, including a qualitative evaluation of the real-time processing capacity of the simulation tool.

II. Framework Components of Current Implementation

Inherent hydraulic actuator dynamics may prevent a calculated analytical substructure displacement from being applied accurately to an experimental substructure. Modeling and compensation of these dynamics are essential features for successful conduct of a RTHT. An MR damper is a type of highly nonlinear device that is nonetheless promising for use

in structural vibration control applications. Reliable damper models are therefore necessary, to develop baselines that can be used to validate and interpret results obtained from an RTHT framework. In our approach, a Linear Quadratic Gaussian (LQG) scheme with acceleration feedback is used as the primary controller to regulate structural response, with a clipped optimal secondary controller to drive the MR damper. A simulation tool used as analytical substructure is introduced at the end of this section.

A. Hydraulic actuator dynamics and compensation

One of the main challenges in conducting a successful and accurate RTHT is to synchronize the displacement and force at each interface between both numerical and experimental substructures. Although inevitable computation and communication delays are observed among various cyber and physical components, experimental studies [1] reveal that the phase lag associated with hydraulic actuator dynamics contributes the largest portion to this apparent delay in the time domain.

Extensive research has been performed to model and compensate actuator dynamics via a suitable control scheme. By simplifying the actuator model as a constant time delay device, a polynomial function based predictive approach was proposed [6] to compensate for delay by extrapolating command displacement values using an n^{th} order polynomial function. Chen [2] proposed a simple delay model by idealizing linear actuator displacement response within each time step. The inverse of this model is therefore used for actuator delay compensation. A model reference adaptive control [7] strategy is applied with the assumption that the plant (actuator dynamics) can be approximated by a first-order transfer function system.

A model based compensation strategy is adopted for the verification experiment in this study. The scheme is based on the dynamic models developed [8] for associated actuator components. The basic mechanism of a servo hydraulic actuator is that the valve receives a current input i_c from controller which creates the spool valve displacement x_v.

$$\tau_v \dot{x}_v = -x_v + k_v \cdot i_c \tag{1}$$

Controlled hydraulic flow Q_L due to spool displacement causes pressure difference P_L inside actuator chambers that will further induce the piston displacement x_m.

$$Q_L = K_q^{'} x_v - K_c^{'} p_L \tag{2}$$

The continuity equation (conservation of mass flow) essentially governs the behavior of the hydraulic actuator.

$$Q_L = A\dot{x}_m + C_l p_L + V_t/(4\beta_e)\dot{p}_L \tag{3}$$

Parameters of the above equations are defined as follows: k_v is the valve gain, τ_v is the servo-valve time constant, K_q' is the valve flow gain, K_c' is the valve flow-pressure gain, A is the area of the piston, C_l is the total leakage coefficient of the piston, V_t is the total volume of the fluid under compression in both actuator chambers and β_e is the effective bulk modulus. Command displacement x_c is applied by an inner-loop PID controller *(P* gain only in this specific experiment),

$$x_c - x_m = K_p \cdot i_c \tag{4}$$

and equilibrium of force is governed by the equation of motion:

$$f_p = p_L \cdot A = m_t \ddot{x}_m + c_t \dot{x}_m + k x_m \tag{5}$$

where m_t, c_t, and k are the mass, damping and stiffness of the piston plus the testing specimen. A feed-forward compensation scheme [1] is thus proposed based on this linear system model which essentially consists of the inverse of the actuator model in series with a unit gain low pass filter.

$$G_C(s) = \alpha^n \cdot \prod_{i=1}^{n}(s - p_{p,i}) / \prod_{i=1}^{n}(s - \alpha \cdot p_{p,i}) \tag{6}$$

where $p_{p,i}$ are poles of the actuator and α is the control variable for the low pass filter.

B. MR damper modeling

An MR damper is a kind of semi-active control device that requires much less energy consumption to operate when compared to active control devices. An MR damper's operation is based on controllable MR fluids. MR fluids have the ability to change from a free-flowing, linear, viscous fluid condition to a semi-solid condition in milliseconds when exposed to a magnetic field. Among various mathematical models for characterizing MR dampers, a phenomenological Bouc-Wen model [12] is used as the simulation model to validate experimental results in this study.

C. Semi-active control strategy

The H_2/LQG algorithm is a disturbance rejection scheme which has been successfully applied in the structural control community for vibration mitigation applications [4]. State space formulation of a linear structure system can be constructed as:

$$\begin{aligned} \dot{z} &= Az + Bf + G\ddot{x}_g \\ y &= Cz + Df + H\ddot{x}_g + v \end{aligned} \tag{7}$$

where state variable vector z includes displacement and velocity on each discrete mass location. Output variable y can be any linear combination of states (e.g. accelerations for estimation of full states) and v is the measurement noise. Matrix coefficients are

$$\begin{aligned} A &= \begin{bmatrix} 0 & I \\ -M_S^{-1}K_S & -M_S^{-1}C_S \end{bmatrix}, B = \begin{bmatrix} 0 \\ M_S^{-1}\Lambda \end{bmatrix}, \mathrm{G} = \begin{bmatrix} 0 \\ -\Gamma \end{bmatrix} \\ C &= \begin{bmatrix} -M_S^{-1}K_S & -M_S^{-1}C_S \end{bmatrix} D = \begin{bmatrix} M_S^{-1}\Lambda \end{bmatrix}, \mathrm{H} = \begin{bmatrix} -\Gamma \end{bmatrix} \end{aligned} \tag{8}$$

and M_s, C_s, and K_s are the mass, damping and linear stiffness of the structure respectively. Γ is the vector considering structure mass influence and Λ is the matrix considering control force f interactions and is determined by the control device placement in the structure.

The control law f=-K·z is achieved by minimizing the quadratic cost function

$$J = E\left\{\int_0^\infty (y^T Q y + f^T R f)dt\right\} \tag{9}$$

where Q and R are weighting matrices to define the tradeoff between regulated responses and control efforts. In practice it is not always feasible to measure all state variables directly, so Kalman state estimator $\hat{z}$ is then constructed to minimize the steady state error covariance

$$\lim_{t\to\infty} E(\{z-\hat{z}\}\{z-\hat{z}\}^T) \tag{10}$$

The nominal control force needs to be applied by physical MR damper devices which take the input voltage as a control variable. Dyke et al. [4] proposed a clipped-optimal strategy as the secondary controller for acceleration feedback control of an MR damper. The voltage applied to each MR damper v_i is determined by the comparison of nominal desired control force f_{di} and measured force f_{mi}

$$v_i = v_{\max} H\{(f_{di} - f_{mi}) \cdot f_{mi}\} \tag{11}$$

where v_{max} is the voltage to the current driver associated with saturation of the magnetic field in the MR damper, and $H\{\cdot\}$ is the Heaviside step function.

D. Simulation tool

Another key component to ensure an adequate RTHT implementation is the ability of the computational tool to recreate the physical behavior of the simulated portion of the test with sufficient accuracy. Additionally, the computational tool must have intensive execution capabilities to guarantee robust compatibility between simulated and experimental components during testing.

Herein, a compatible version of a MATLAB-based simulation tool [10] adequate to be compiled and executed under the real-time kernel platform used in this study (section III-A), is proposed as the simulation tool. This simulation tool, developed for analysis of seismically excited non-linear buildings, has been used throughout the community for a benchmark control problem [11] and been verified through comparison with the structural analysis program IDARC2D [14]. The tool implements a bilinear hysteresis model with a kinematic hardening rule to recreate yielding locations that are assumed to occur at the moment resisting connections of steel buildings.

The bilinear properties can be predefined for each structural element depending on the selected section. The yielding location can be represented with either a spread plasticity model (SPM) or a concentrated plasticity model (CPM), where yielding is limited only to the ends of the member while the interior is assumed to be elastic [3, 5]. In the SPM, a simple supported beam model is utilized for derivation of the 2x2 stiffness matrix relating moments and rotations at ends as follows:

$$\begin{bmatrix} M_A \\ M_B \end{bmatrix} = \tilde{K}_S \begin{bmatrix} \theta_A \\ \theta_B \end{bmatrix} = \begin{bmatrix} k_{AA} & k_{AB} \\ k_{BA} & k_{BB} \end{bmatrix} \begin{bmatrix} \theta_A \\ \theta_B \end{bmatrix} \tag{12}$$

where:

$$k_{AA} = \frac{12EI_0 EI_A EI_B}{D_{et} L}\left(f'_{BB} GA_Z L^2 + 12EI_0 EI_A EI_B\right)$$

$$k_{AB} = k_{BA} = -\frac{12EI_0 EI_A EI_B}{D_{et} L}\left(f'_{AB} GA_Z L^2 + 12EI_0 EI_A EI_B\right)$$

$$k_{BB} = \frac{12EI_0 EI_A EI_B}{D_{et} L}\left(f'_{AA} GA_Z L^2 + 12EI_0 EI_A EI_B\right)$$

$$f'_{AA} = 4EI_A EI_B + (EI_0 - EI_A)EI_B(6\alpha_A - 4\alpha_A^2 + \alpha_A^3) + (EI_0 - EI_B)EI_A\alpha_A^3$$

$$f'_{AB} = -2EI_A EI_B - (EI_0 - EI_A)EI_B(2\alpha_A^2 - \alpha_A^3) - (EI_0 - EI_B)EI_A(2\alpha_B^2 - \alpha_B^3)$$

$$f'_{BB} = 4EI_A EI_B + (EI_0 - EI_A)EI_B\alpha_A^3 + (EI_0 - EI_B)EI_A(6\alpha_B - 4\alpha_B^2 - \alpha_B^3)$$

$$D_{et} = GA_Z L^2 (f'_{AA} f'_{BB} - f'^{\,2}_{AB}) + 12EI_0 EI_A EI_B (f'_{AA} + f'_{BB} - 2f'_{AB})$$

GA and L are the shear stiffness and the length of the member, respectively. EI_A and EI_B are the instantaneous flexural stiffness at the member end sections, whose values are progressively updated from the hysteresis model. α_A, α_B and EI_0 are yield penetration parameters and flexural stiffness at the center of the member, respectively. The yield penetration parameters are functions of the moment distribution and previous yield penetration history. Therefore, the 4x4 element stiffness matrix $\tilde{K}_e$ can be derived by using the equilibrium matrix between shear forces and moments as:

$$[V_A \quad M_A \quad V_B \quad M_B]^T = \tilde{R}_e [M_A \quad M_B]^T \tag{13}$$

where, $\tilde{K}_e = \tilde{R}_e \tilde{K}_S \tilde{R}_e^T$

Additionally, an unconditional stable Newmark-type integration scheme [9] is adopted in conjunction with the pseudo-force method [13] to solve the incremental equation of motion and evaluate the non-linear response. After substituting the corresponding Newmark's equations with parameters β=1/4 and γ=1/2 into the incremental equation of motion, the resulting expression to solve for the displacement increment $\Delta\tilde{U}$ is:

$$\tilde{K}_D \Delta\tilde{U} = \Delta\tilde{F}_D \tag{14}$$

where:

$$\tilde{K}_D = \frac{1}{\beta(\Delta t)^2}\tilde{M} + \frac{\gamma}{\beta(\Delta t)}\tilde{C} + \left[\tilde{K}_0 + \Delta\tilde{K}\right]$$

$$\Delta\tilde{F}_D = -\tilde{M}\tilde{G}\Delta\ddot{x}_g + \left[\frac{1}{2\beta}\tilde{M} + (\frac{\gamma}{2\beta} - 1)\Delta t\tilde{C}\right]\ddot{\tilde{U}}_t + \left[\frac{1}{\beta\Delta t}\tilde{M} + (\frac{\gamma}{\beta})\tilde{C}\right]\dot{\tilde{U}}_t + \tilde{P}\Delta f + \Delta\tilde{F}_{err}$$

$\tilde{M}, \tilde{C}, \tilde{K}$ are the global lumped mass, Rayleigh damping and stiffness matrices, respectively. $\dot{\tilde{U}}_t, \ddot{\tilde{U}}_t$ are the velocity and acceleration vectors at time t. $\Delta\ddot{x}_g, \Delta f$ are the ground

acceleration and control force increments, respectively. $\widetilde{G}, \widetilde{P}$ are the loading vectors for ground motion and control forces, respectively. $\Delta\widetilde{F}_{err}$ is the vector of unbalanced forces. The unbalanced force is the force-difference between the restoring force evaluated using the hysteretic model and the one calculated by assuming a constant linear stiffness at time t during the time interval t ~ t+Δt. This unbalanced force is added into the equation of motion at the next time step as an external pseudo-force.

In section IV, a preliminary evaluation of the performance of the proposed simulation tool under real-time processing conditions is presented and discussed.

III. Experimental Components

A. Real-time kernel platform

Our RTHT algorithm development for this work is based on MATLAB/SIMULINK [15]. The xPC Target is a flexible real-time testing solution that combines target machine and I/O modules that can both be chosen from a large variety of hardware options. Generated code is downloaded from a host computer onto a target kernel machine and executed directly atop the target machine hardware. The target machine for this experiment is a standard desktop PC with a Pentium IV 2.6 GHz processor and 512 MB memory. The I/O device used is a NI PCI-6251 multifunction DAQ board with a resolution of 16 bits that supports a maximum sample rate of 1.25 MS/s.

B. Servo-controller and actuator

The Bowen lab at Purdue University houses a MTS hydraulic pump that can be operated at 3,000 psi with a maximum flow rate of 120 GPM. Flow passes through a hydraulic manifold rated at 60 GPM and 3000 psi oil service. A Shore Western SC6000 analog controller in displacement feedback control mode accepts desired trajectory calculated from target PC, then apply it on a Shore-Western 910D double-ended hydraulic actuator to drive the physical test specimen. A Schenck Pegasus 162M servo-valve rated for 15 GPM at a 1,000 psi pressure drop is used to control the actuator. The servo-valve has a nominal operational frequency range of 0-60 Hz. An Omega LC101-1k load cell with a range of 1 kip is included in series with the physical test specimen to measure the corresponding force at the interface between numerical and physical substructures.

C. MR damper specimen

The experimental substructure for this study is composed of a MR damper specimen that is 8.5in long in its extended position with an operational stroke of +/- 1 in. The main cylinder, with a 1.5 in diameter, contains the MR fluid, the magnetic circuit and the piston. The magnetic field can be varied from 0 to 200 kA/m by applying currents of 0 to 1 amp in the electromagnet coil. The peak power required is less than 10 watts, which allows the damper to be operated continuously for more than an hour on a small camera battery. With this device, forces up to 675 lb are expected to be achieved under small variations over a broad temperature range (less than 10%).

A series of tests is conducted to measure the damper response under various loading conditions to characterize the proposed damper model. Comparison between the experimentally measured responses and the Bouc-Wen model are presented in Figure 1. A 5 Hz sinusoidal displacement command (a) with amplitude of 0.2 in is tested for both cases with constant voltage of 0V and 3V respectively. Band-limited white noise displacement input (b) is also tested at RMS amplitude of 0.1 in and band width of 10 Hz. The excellent match in all cases demonstrates the effectiveness of the identified model to represent the physical device.

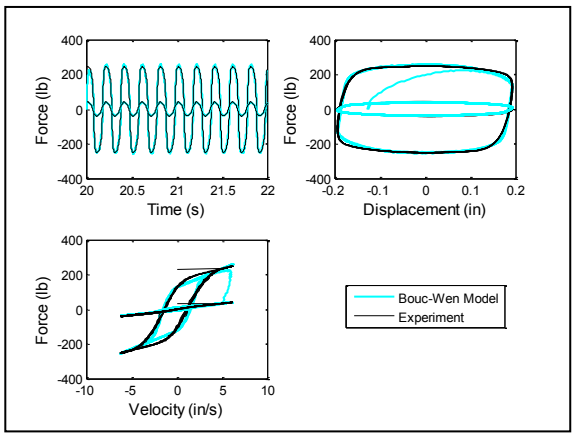

(a) sinusoidal command

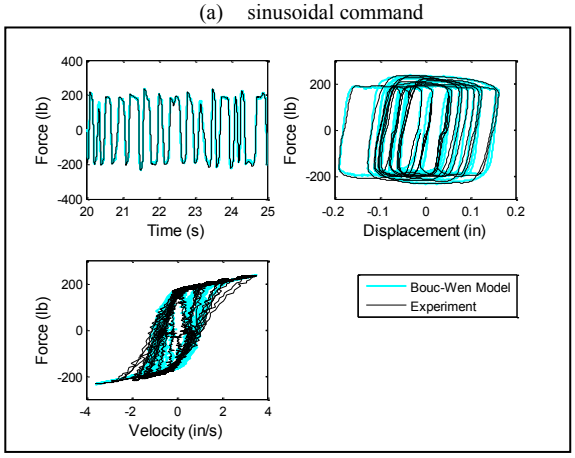

(b) band limited white noise command

Fig. 1. Comparison of MR damper response with Bouc-Wen model

D. Numerical substructure model

A 2D two-story-one-bay steel frame numerical model is utilized as the analytical sub-structure component in the experimental validation. Nonlinear frame elements, in agreement with the concentrated plasticity formulation, are used to model the beam members while linear elastic frame elements are used for the columns. A moment-curvature bilinear hysteresis model for the beam-column connections is defined with a post-yielding stiffness reduction of 90% with respect to the original flexural stiffness. Additional to a regulated non-linear response, member sections and mass distribution are designed in accordance to the force operational range of the damper device. Each story has a dimension of 19.7 in and the bay width is 23.6 in, defining a total height to width aspect ratio of H/W=1.67. Columns are

designed with rectangular cross section members of 2 in x 5/4 in placed under a continuous length format so that no column-column connections (splices) are utilized. Likewise, beams are designed with rectangular cross section members of 1 in x 1/2 in. Inertial effects are accounted for by a lumped mass matrix approach with a mass distribution of 7.14 lb-s^2/in per floor. The damping matrix is determined based on an assumption of Rayleigh damping with a critical modal damping ratio of 2%. Finally, boundary conditions at the column supports are assumed to be fixed in translation and rotation. The resulting analytical model leads to a 6 nodes – 12 active global degrees of freedom - system with natural frequencies corresponding to the first and second mode of 2.00 Hz and 11.75 Hz respectively.

IV. Experimental Validation

A. Real-time processing evaluation of simulation tool

A preliminary evaluation of the real-time processing capacity of the proposed simulation tool is presented in this section. Non-linear dynamic analyses of 3-story-one bay (Model 1), 4-story-two bay (Model 2), 3-story-four bay (Model 3), 9-story-five bay (Model 4) and 20-story-five bay (Model 5) building models were performed using a real time processor. Every structural scenario was subjected to the N-S earthquake record component measured at the Kobe Japanese Meteorological Agency (JMA) station during the Kobe earthquake of January 17, 1995. The target system mentioned in section III-A is used to evaluate every scenario. Table I shows the corresponding maximum sampling frequencies that the simulation tool is able to achieve for each of the proposed cases. Successful real-time performance is reached for the Models 1, 2, and 3, since sampling frequencies much greater than 1024 Hz are achieved. (1024 Hz sampling frequency value is used as reference since it is commonly accepted for most of the RTHT implementations). Conversely, when the structural complexity increases by a considerable amount (in the number of DOF), a substantial decrease in the sampling frequency is observed (Models 4 and 5).

TABLE I
REAL TIME PROCESSING EVALUATION

Model	# Degree of Freedom	Maximum Fs (Hz)
1	18	10000
2	45	2200
3	45	2000
4	180	125
5	396	25

B. RTHT validation

Verification experiments were conducted using the nonlinear structural model and MR damper devices described in section III. The structure is subjected to half intensity of the NS component of the 1940 El Centro earthquake with the MR damper experimental setup shown in Figure 2.

The model based compensation scheme requires knowledge of actuator dynamics *a priori* in order to generate effective control. The transfer function between the input command displacement x_c and output measurement x_m are experimentally obtained. The displacement input is chosen as a band-limited white noise from 0-50 Hz with RMS amplitude of 0.03 in. The sampling frequency of the system is set to be 1024 Hz and the transfer function is calculated with 4096 FFT points. Successive sections are Hanning windowed with 50% overlap and 50 averages. Two experimental transfer functions are obtained separately when the damper is subject to 0V and 3V. The MR damper needs to be operated under rapid voltage switches in typical semiactive control applications, and thus it is important to have a compensation scheme that is robust to account for such actuator dynamic changes at variable input voltages. The model based compensation scheme is thus further developed [1] by adding a bumpless transfer element G_T where τ_t determines the speed and smoothness of transition

$$G_T(s) = 1/[V_{\max} \cdot (\tau_t s + 1)] \quad (15)$$

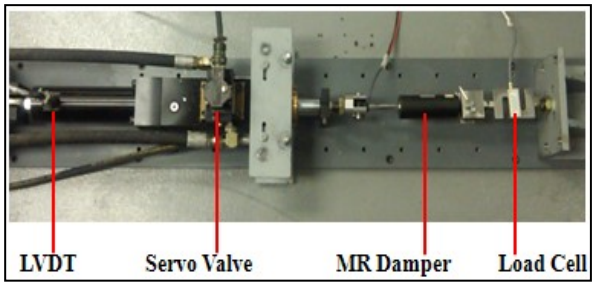

Fig. 2. Validation test experimental Setup

Four different control cases are considered here: (1) an uncontrolled case (structure without the MR damper) (2) a passive off case (the MR damper is used as a passive device with constant 0 input voltage) (3) a Passive on case (the MR damper is used as a passive device with constant maximum input 3V) and (4) a Semiactive case (voltage to the MR damper device varies and is determined by the clipped optimal control algorithm described in section II-C). The Bouc-Wen model is implemented as a continuous dynamic system in SIMULINK and evaluated by a Runge-Kutta numerical integration solver with a fixed time step of 1024 Hz. Compensation feed-forward gain is taken as α=3 and τ_t=0.0048. The semiactive controller is designed by placing a high weighting on both floor displacements.

A comparison of 1st story displacement responses from the experiment and the simulation is presented in Figure 3. Only the first 20s results are considered since the peak responses occur during this portion of the earthquake. Excellent agreement is observed for all three control cases, which demonstrates the capability of the developed framework for conducting RTHTs. The uncontrolled simulation response is also included in the semiactive control plot to demonstrate the effectiveness of the semiactive controller in mitigating structure vibration. RMS structure responses (shown in Table II) provide a direct comparison. The semiactive controller performs better than both passive cases and reduces approximately 40% of structure displacement compared with the uncontrolled case in this particular application.

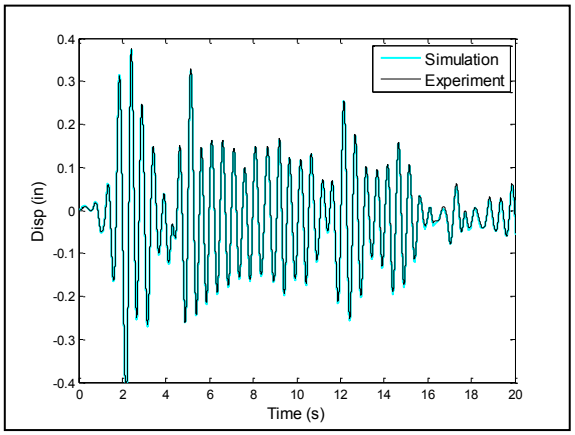

(a) passive off

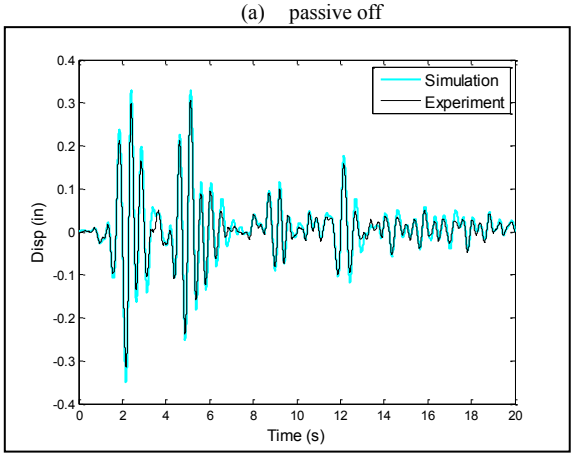

(b) passive on

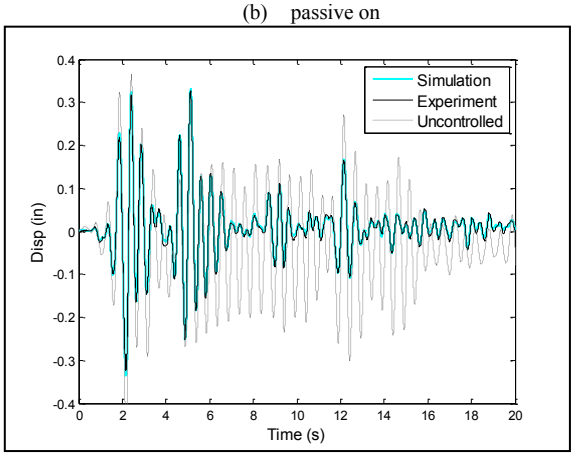

(c) semiactive vs. uncontrolled

Fig. 3. Comparison of RTHT and simulation response

TABLE II
RMS VALUE OF STRUCTURE DISPLACEMENT

	1st floor (in)	2nd floor (in)
Uncontrolled	0.1233	0.3676
Passive off	0.1133	0.3384
Passive on	0.0749	0.2259
Semiactive	0.0736	0.2239

V. SUMMARY

We are developing hardware and software components to build an innovative instrument to perform real-time hybrid testing of structural systems. A successful validation experiment was conducted to demonstrate the effectiveness and efficiency of the current stage of development. Our future plans include developing advanced adaptive and robust algorithms that can handle model uncertainties in physical substructure testing, further validating the platform for more realistic and complicated MIMO structure testing; accommodating distributed computational resources in real-time testing; and designing and implementing more user friendly visualization and control tools. An improved version of the proposed computational tool with more advanced simulation capabilities will be available as an open-source tool in the near future.

REFERENCES

[1] Carrion, J. E. and Spencer, B. F. (2007), "Model-based strategies for real-time hybrid testing." Newmark Structural Engineering Laboratory Report Series, University of Illinois at Urbana-Champaign, Urbana, IL, No. 6.

[2] Chen, C. (2007), "Development and numerical simulation of hybrid effective force testing method." Ph.D. dissertation, Dept. of Civil and Environmental Engineering, Lehigh Univ., Bethlehem, Pa.

[3] Clough, R.W. and Johnson, S. (1966). "Effect of stiffness degradation on earthquake ductility requirements." Proc. of the Japan Earthquake Engineering Symposium, Tokyo.

[4] Dyke, S.J., Spencer, B. F., Sain, M. K. and Carlson, J. D. (1996), "Modeling and Control of Magnetorheological Dampers for Seismic Response Reduction", Smart Structures and Materials, 5(5), pp. 565-575.

[5] Giberson, M.F. (1967). The response of nonlinear multistory structures subjected to earthquake excitation. Ph.D. Dissertation, Caltech.

[6] Horiuchi, T., Inoue, M., Konno, T. and Namita, Y. (1999), "Real-Time Hybrid Experimental System with Actuator Delay Compensation and its Application to a Piping System with Energy Absorber." Earthquake Engineering and Structural Dynamics, 28(10), pp. 1121-1141.

[7] Lim C. N., Neild S. A., Stoten D. P., Drury D and Taylor C. A. (2007), "Adaptive control strategy for dynamic substructuring tests", Journal of Engineering Mechanics, 113(8), pp. 864-873.

[8] Merritt, H. E. (1967). Hydraulic control systems. Wiley, New York.

[9] Newmark, N.M. (1959) "A method of computation for structural dynamics" Journal of Engineering Mechanics Division, ASCE, Vol. 85, pp.67–94.

[10] Ohtori, Y. and Spencer, B.F., Jr. (1999). "A MATLAB-Based Tool for Nonlinear Structural Analysis", In the Proceedings of the 13th ASCE Engineering Mechanics Division Specialty Conference, Johns Hopkins University, Baltimore, June 13-16.

[11] Ohtori, Y., Christenson, R.E., Spencer, B.F. and Dyke, S.J. (2004). "Nonlinear Benchmark Control Problem for Seismically Excited Buildings". ASCE Journal of Engineering Mechanics, 130(4), pp.366-385,2004

[12] Spencer, B. F., Dyke, S. J., Sain, M. K., and Carlson, J. D. (1997), "Phenomenological model for magneto rheological dampers", Journal of Engineering Mechanics, ASCE, 123(3): pp. 230-238.

[13] Subbaraj, K. and Dokainish, M.A. (1989). "A Survey of Direct Time-Integration Methods in Computational Structural Dynamics - II. Implicit Method." Computers and Structures, Vol.32, No.6, pp.1387–1401.

[14] Valles, R.E., Reinhorn, A.M., Kunnath, S.K., Li, C. and Madan, A. (1996). "IDARC2D Version4.0: A Computer Program for the Inelastic Damage Analysis of the Buildings." Technical Report NCEER-96-0010, Nat. Ctr. for Earthquake Engrg. Res., Buffalo, New York.

[15] http://www.mathworks.com/